TABLE 2: Developmental Milestones and Clinical Course

Patient	Age at Last Investigation	Head Control	Walked Alone	Muscle Weakness	Gavage Feeding (age)	Respirator (age)	CK, Lactate Data	Complications
1	15 yr	Unknown	2 yr 0 mo	(–)	(–)	(–)	ND	None
2	11 yr	8 mo	2 yr 8 mo	(–)	3–4 mo	(–)	Normal after 3 yr; transient mild elevated serum CK and lactate during infection	None
3	11 yr	Unknown (roll over 9 mo)	Late infancy	Mild exercise intolerance (walking for long time or climbing)	(–)	(–)	ND	None
4	5 yr	9 mo	1 yr 3 mo	(–)	(–)	2–6 mo	Normal at the age of 1 yr 10 mo	None
5	6 yr	10 mo	12 mo	(–)	0–2 d	(–)	ND	Febrile convulsion (2 yr)
6	1 yr 6 mo	9 mo	1 yr 6 mo	Mild muscle weakness	(–)	(–)	Normal after 11 mo	None
7	4 yr	8–9 mo	1 yr 4 mo	(–)	(–)	(–)	Normal after 2 yr 11 mo	None
8	3 yr	7 mo	1 yr 4 mo	(–)	(–)	(–)	Normal after 2 yr	None

CK = creatinine kinase; ND = not determined.

Results

Clinical Features

Profound generalized muscle hypotonia and weakness occurred between birth and 3 months of age. Involvement of facial muscles with a high-arched palate was noted in 2 patients (see Table 1). The clinical diagnoses prior to muscle biopsy were mitochondrial myopathy in 5 patients, congenital myopathy in 2, and congenital muscular dystrophy in 1.

Review of clinical course after muscle biopsy or DNA analysis (Table 2) showed that all patients, except patient 6, recovered to an almost normal state during the 3-year follow-up period. Patients 2 and 5 required tube feeding during early infancy, and patient 4 was on a respirator from 2 to 6 months of age. All learned to walk by 1–2 years of age and could run normally when they were last examined. Although patient 6 had a slight delay in gross motor developmental milestones at 18 months of age, he could walk without support. No patient had short stature, renal dysfunction, liver dysfunction, cardiomyopathy, or diabetes mellitus.

Laboratory Findings

Blood lactate levels were normal in 2 patients, slightly elevated (20–25 mg/dl) in 4, and more than twice the

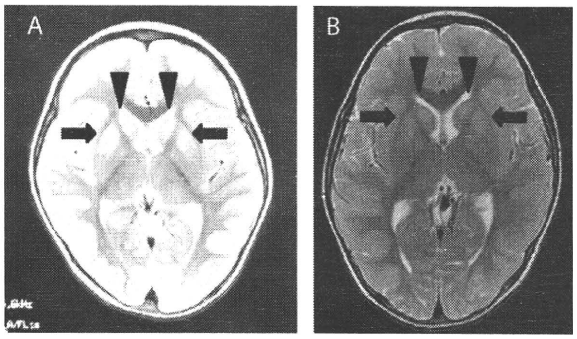

FIGURE 1: Brain MRI images of (A) patient 7 at the age of 23 months and (B) patient 8 at the age of 33 months. Abnormally high T2-weighted signals in bilateral caudate nuclei *(arrowheads)* and putamina *(arrows)*.

normal level in 2 (see Table 1). Patient 4 had high blood and CSF lactate levels during early infancy, but the levels subsequently normalized. Serum CK levels during infancy were elevated in all patients (range, 182–644 U/L; mean, 366 U/L) and reached normal levels with development. In patients 7 and 8, brain magnetic resonance imaging (MRI) images revealed abnormally high T2-weighted signals in bilateral caudate nuclei and putamina at the age of 23 months (Fig 1A) and 33 months (see Fig 1B), respectively, although these signals had been previously normal at the age of 7 months and 13 months, respectively. Brain CT and MRI images performed in 2 other patients were normal.

Muscle Pathology

All biopsy specimens showed marked variation in fiber size. There were numerous ragged-red fibers (RRFs) in all specimens, comprising 5% to 25% of fibers (Fig 2A). RRFs frequently had oil-red O-positive vacuoles and stained strongly on periodic acid-Schiff (PAS). There was

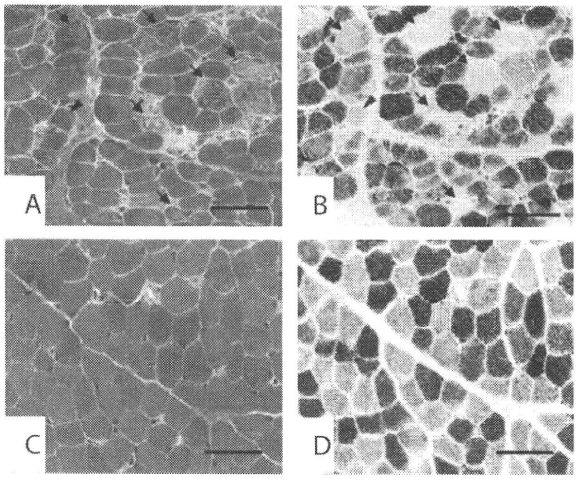

FIGURE 2: Representative muscle pathology. Patient 6 (A, B) and age-related control (aged 1 year and 3 months) without mitochondrial disease (C, D). Serial sections are stained with modified (A, C) Gomori trichrome and (B, D) COX stains. The muscle of the patient had marked fiber-size variation and numerous basophilic RRFs. RRFs *(arrows)* are always COX-deficient, and the fibers of normal appearance *(arrowheads)* are sometimes COX-deficient. Bar = 50μm.

no obvious strongly SDH-reactive blood vessel and no abnormal blood vessel under light microscopy.[31] In all specimens, scattered muscle fibers were faintly positive to normal COX activity with focal deficiency (see Fig 2B). RRFs were always COX-negative. In several specimens, a portion of normal-appearing type 1 fibers (non-RRF) also showed reduced activity (see Fig 2A, B). COX activity of intrafusal fibers, small arteries, and intramuscular peripheral nerves appeared normal (see Table 1).

mtDNA Analysis

No large-scale mtDNA rearrangements were detected by long PCR and Southern methods. Total mtDNA

TABLE 3: Total Sequence Analysis of mtDNA

Gene/Patient	ND1	ND1	COI	ATP8	ATP8	ND4	$tRNA^{Glu}$	$tRNA^{Glu}$	D-loop
1								T14674G	C16197T
2		C3408T					C14067T	T14674C	
3					C8409T	A8459G			T14674G	
4								T14674C	
5			G3496T	T6185C				T14674C	
6								T14674C	
7								T14674C	
8								T14674C	

Fifteen polymorphisms were revealed that were not detected in 100 normal subjects. We identified homoplasmic mutations at np 14674 in the mitochondrial $tRNA^{Glu}$ in all 8 subjects. Patients 1 and 3 had the T14674G mutation and patients 2, 4, 5, 6, 7, and 8 had the T14674C mutation, neither of these mutations were detected in 200 normal controls.

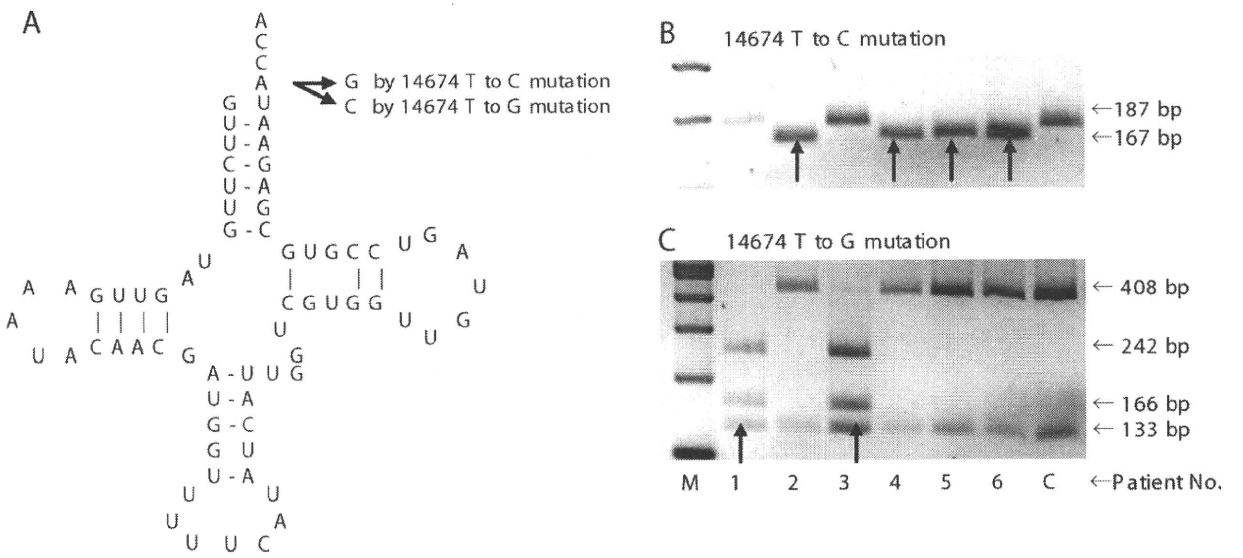

FIGURE 3: (A) Mutations at the discriminator base of $tRNA^{Glu}$. Nucleotide position 14674 is the discriminator identified by the aminoacyl-tRNA synthetase. The arrows show the A to G mutation by m.14674T>C and the A to C mutation by m.14674T>G. The CCA sequence is added to the nucleotide before this tRNA charges glutamate. (B) Identification of m.14674T>C mutation in mtDNA. The 187-bp PCR fragments with the mismatched and reverse primers were digested by *BclI*. Wild-type mtDNAs are indicated by 187-bp bands and mutant mtDNAs are indicated by 167-bp bands in patients 2, 4, 5, and 6 *(arrows)*. (C) Identification of m.14674T>G mutation in mtDNA. The amplified 541-bp PCR fragments were digested by *NlaIII*. Wild-type mtDNAs are indicated by cleaved fragments of 408bp and 133bp, and mutant mtDNAs are indicated by 133-bp, 242-bp, and 166-bp bands divided from the 408-bp bands in patients 1 and 3 *(arrows)*. Each fragment was detected on a 4% agarose gel and visualized with ethidium bromide under UV light.

sequencing from these patients revealed many polymorphisms. Most were silent mutations or reported as normal polymorphisms according to a human mitochondrial genome database (MITOMAP).

Fifteen base changes were not present in 100 normal Japanese adults (Table 3). In the reported polymorphisms, patients 2, 4, 5, 6, 7, and 8 had previously reported T to C base change at np 14674 in the $tRNA^{Glu}$. Furthermore, patients 1 and 3 had a T to G base change at the same np (np 14674) in the mitochondrial $tRNA^{Glu}$ gene, which has not been previously reported according to the MITOMAP database (Fig 3A). These base changes were confirmed by RFLP analysis and revealed to be homoplasmic (see Fig 3B, C; data for patients 7 and 8 not shown).

Mitochondrial tRNA Analysis

In northern blot analysis using total RNA extracted from muscle specimens of patients and normal infants, values were normalized by the amount of mitochondrial tRNA-Leu (UUR) and nuclear-encoded 5S rRNA as internal standards. The $tRNA^{Glu}$ molecules in patients were the same size as those in normal infants. However, the amount of $tRNA^{Glu}$ in patients was about one-fourth of that in normal controls. The amount of tRNA-Leu (UUR) in patients and normal infants remained unchanged (Fig 4).

By acid PAGE, the degrees of delay in electrophoresis of cybrids or naive myoblasts derived from patient 6 were identical to those of normal control 143B/TK-cells (Supporting Information Fig S1). This finding suggested that aminoacylation of $tRNA^{Glu}$ from patients carrying the mutation was normal and glutamate was correctly charged to tRNA.

Biochemical Studies

Respiratory chain enzyme assay of skeletal muscle showed that complex IV activity in patients 3, 4, and 6 and

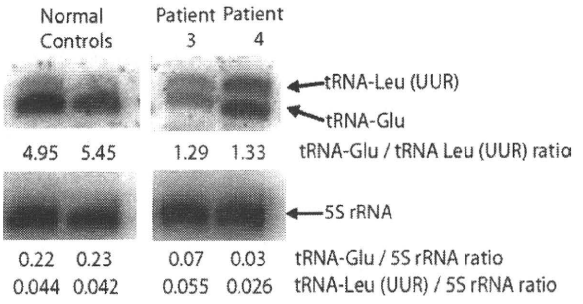

FIGURE 4: Quantitative analysis of $tRNA^{Glu}$ in muscle. Total RNA was extracted from patients 3 and 4 as well as from the muscle specimen of 2 normal infants (normal controls). The same amount of each RNA sample was electrophoresed followed by northern hybridization. The amounts of $tRNA^{Glu}$ were normalized by the amount of mitochondrial tRNA-Leu (UUR) and nuclear-encoded 5S ribosomal RNA. The amount of $tRNA^{Glu}$ in patients was about one-fourth that in normal controls, although the amount of tRNA-Leu (UUR) remained unchanged in both patients and normal infants.

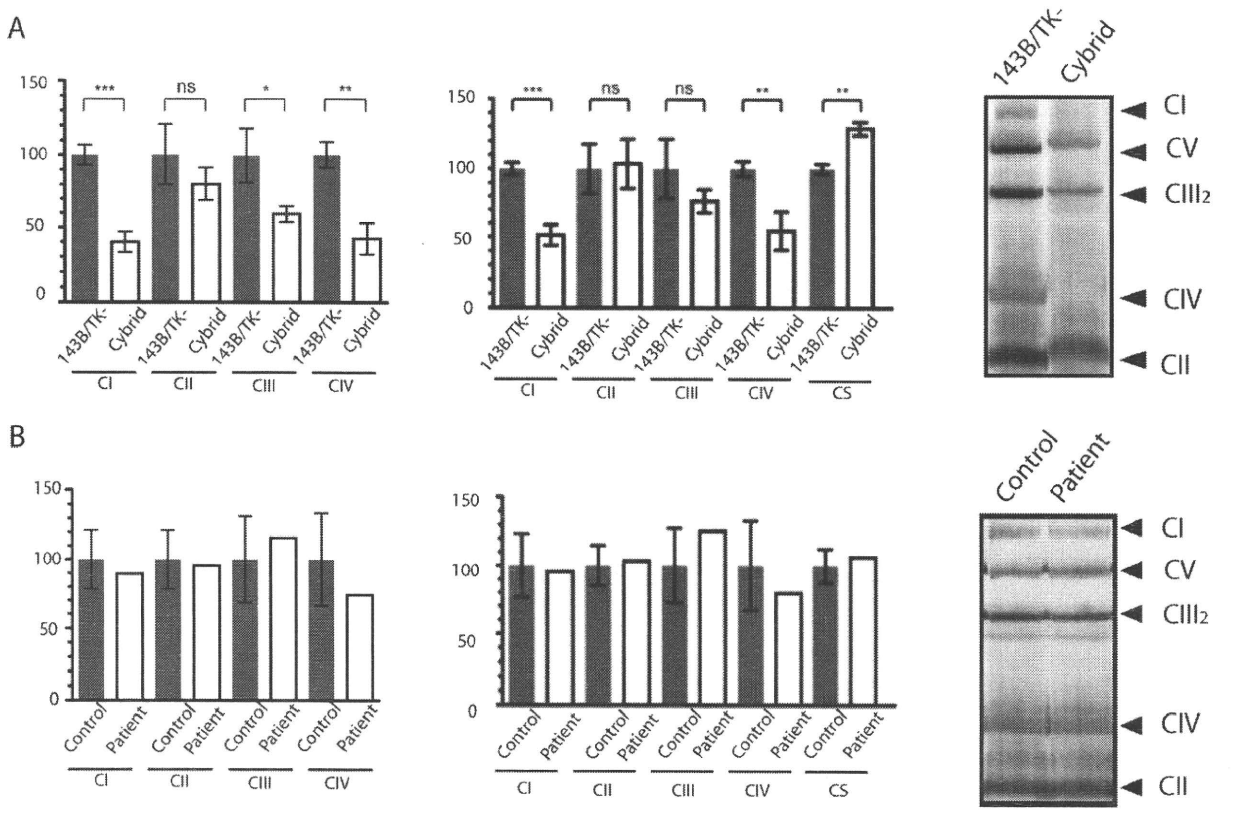

FIGURE 5: Respiratory chain enzyme assay and BN-PAGE of (A) cybrids derived from patient 6 compared with 143B/TK-cells and (B) naive myoblasts derived from patient 6 compared with normal control myoblasts. Enzyme activities are expressed as percent of mean normal control activity relative to protein and CS. Cybrids showed reduced levels of complexes I, III, and IV relative to protein and reduced levels of complexes I and IV relative to CS. BN-PAGE also revealed a severe decrease in the amount of complexes I and IV. Naive myoblasts of patient 6 showed normal respiratory chain enzyme activities and normal amounts of respiratory complex enzymes in BN-PAGE. BN-PAGE = blue native polyacrylamide gel electrophoresis; CS = citrate synthase.

complex I activity in patients 4 and 6 apparently decreased (see Table 1). The activities of complexes II and III relative to protein were within normal limits, while those relative to citrate decreased because CS activity increased.

To confirm the pathogenicity of the m.14674T>C mutation, respiratory chain enzyme assay and BN-PAGE were performed on mitochondrial proteins isolated from cybrids derived from patient 6 and 143B/TK-cells. In respiratory chain enzyme assay, cybrids showed reduced levels of complexes I, III, and IV relative to protein and reduced levels of complexes I and IV relative to CS compared with 143B/TK-cells. BN-PAGE also revealed a severe decrease in the amounts of complexes I and IV (Fig 5A). In contrast, the naive myoblasts of patient 6 showed normal respiratory chain enzyme activities and normal amounts of the respiratory complex enzymes in BN-PAGE (see Fig 5B).

Discussion

We examined 8 cases in 7 independent Japanese families with the reversible clinical phenotype of mitochondrial disorder, which is consistent with "benign COX deficiency myopathy." Recently, homoplasmic m.14674T>C mutation was reported in 17 affected individuals; the authors emphasized the importance of genetic testing to identify infants with this mitochondrial myopathy and predict a good prognosis.[21] In the present study, we identified the mutation in 6 patients. Identification of the same mutation in many Japanese patients supports the premise that detecting the mutation is useful in diagnosing the disease. Muscle specimens from all patients showed typical morphological features of mitochondrial myopathies in accordance with the classical fatal infantile form of COX deficiency, which is phenotypically similar to the benign form at an early stage. Therefore, detection of homoplasmic mutations in blood samples is important and useful for diagnosis of the benign form. In fact, we were able to make a diagnosis and predict a good prognosis for patients 7 and 8 based on mtDNA analyses using blood samples without muscle biopsy. Furthermore, in patients 1 and 3, we identified a novel homoplasmic m.14674T>G mutation. Clinical phenotypes were the same as those of patients carrying the m.14674T>C

mutation, providing further evidence that the mutation at this np is important to disease causation, and not only m.14674T>C but also m.14674T>G mutation should be tested for when clinicians suspect the disease.

In the literature, at least 19 patients have been reported as having "benign COX deficiency myopathy" or a similar disease.[2,15–21,32] Most of these patients showed clinical symptoms in only skeletal muscle and good recovery, which was similar to patients in this and a previous study.[21] However, with regard to the patient reported by Suzuki et al.,[19] who could not stand up at age 22 months and was probably mentally retarded, the tempo of recovery and subsequent disease outcome in such a patient is variable, and thus, the definition of the disease has been unclear. Lack of good recovery may be indicative of other diseases. Detection of m.14674T>C and m.14674T>G mutations should be helpful for redefinition of this disease. We also identified 2 siblings carrying the mutation with bilateral lesions in caudate nuclei and putamina, which are often affected in mitochondrial disorders such as Leigh encephalopathy. Abnormalities outside of muscle may have been overlooked in this disease. Thus we must draw attention not only to muscle, but also to the central nervous system, even at later stages of the disease.

Because the base changes are located at the end of the aminoacyl acceptor stem of $tRNA^{Glu}$, which plays an important role in tRNA identity as the discriminator base,[33] abnormality of the amino acid charge to tRNA molecule may occur. However, acid PAGE revealed that the aminoacylation ratio of $tRNA^{Glu}$ from a patient carrying the mutation was normal. Therefore, the mutation had no influence on the steady-state level of aminoacylation. However, the muscle specimen from patient 4 carrying the m.14674T>C mutation had 75% less $tRNA^{Glu}$ molecules than specimens from normal infants as previously reported.[21] Furthermore, $tRNA^{Glu}$ molecules of the muscle specimen from patient 3 carrying the m.14674T>G mutation also markedly decreased. Instability and reduction of tRNA molecule carrying a mutation in the corresponding tRNA gene of mtDNA may be responsible for mitochondrial diseases.[34,35] A reduction in the amount of $tRNA^{Glu}$ should be essential to affect translation. COX is a complex enzyme composed of 13 subunits. The 3 larger subunits (I, II, and III) are synthesized in the mitochondria under the direction of mtDNA using the mitochondrial tRNA molecules. It is possible that mtDNA mutation in the mitochondrial $tRNA^{Glu}$ has an influence on the synthesis of 1 of these 3 subunits by reduction of $tRNA^{Glu}$. In particular, subunit II (COXII) gene contains as many as 11 glutamates that constitute 4.8% of total amino acids in COXII, whereas glutamate constitutes 1.9% in the subunit I (COXI) gene and 2.7% in the subunit III (COXIII) gene. It has been reported that fatal infantile COX deficiency was characterized by the selective absence of subunits VIIa+VIIb under the control of nuclear DNA, whereas subunits VIIa+VIIb and COXII encoded by mtDNA in a benign type were absent.[36] The mutation in $tRNA^{Glu}$ gene may cause pathological findings by a translational depression of COXII-containing glutamates in highest proportion among the subunits. These facts indirectly support the pathogenicity of the mutation.

Biochemical analyses in this study revealed some new aspects of this disease. In respiratory chain enzyme assay of skeletal muscle, not only complex IV activity but also complex I activity significantly decreased. It is reasonable to suppose that a reduction in the amount of $tRNA^{Glu}$ should affect translation of not only complex IV but also other respiratory complexes. The activities of complexes II and III relative to CS also decreased because CS activity apparently increased, which suggested that the increase in the number of mitochondria was caused by respiratory enzyme deficiency. Both respiratory chain enzyme assay and BN-PAGE showed defects in complexes I and IV during biochemical studies using cybrids carrying m.14674T>C mutation. This finding directly revealed the pathogenicity of the mutation. Interestingly, naive myoblasts carrying the same mutation showed normal respiratory chain enzyme activities and normal amounts of the respiratory complex enzymes in BN-PAGE. From these facts, it is reasonable to think that nuclear factor(s) may compensate for the defects caused by mtDNA mutation in naive myoblasts through cell division and proliferation during the establishment of the myoblast cell line. The discrepancy between skeletal muscle specimen and myoblasts suggests that the recovery of the respiratory chain enzymes in the skeletal muscle in vivo and clinical symptoms was acquired through the cell proliferation and/or differentiation of myoblasts during the aging or development of the patients. In skeletal muscle in vivo, it is likely that enzyme defects and clinical symptoms become obvious during the early infantile period when compensation is insufficient. Unknown nuclear factor(s) relating to the control of the amount of $tRNA^{Glu}$ may be a key factor in mechanisms of recovery.

Because human mtDNA is maternally inherited, similar abnormalities should be seen in mother and siblings; however, most of the maternal families are asymptomatic. In our case, the mother of patient 6, who did not have a remarkable past history, also carried the m.14674T>C mutation. It seems appropriate to think

that maternal families who have nuclear factors compensating for the defects of the respiratory chain enzymes caused by mtDNA mutation become asymptomatic. In the cases with insufficient compensation, clinical presentations involving not only muscle but also central nervous system may appear, which is similar to our affected siblings.

In summary, we confirmed the pathogenicity of the mutation at np 14674 in $tRNA^{Glu}$ resulting in deficiency of multiple respiratory enzymes. We hypothesize that mtDNA mutation has a great impact on multiple respiratory chain enzyme activities and there should be compensatory mechanisms of nuclear factor(s). According to the degree of compensation, clinical features may vary from asymptomatic maternal families to patients with central nervous system involvement. Our results provide new insights into the disease known as "benign COX deficiency myopathy." We propose that this disease should be renamed "infantile reversible respiratory chain deficiency" as it is caused by deficiency of multiple respiratory chain enzymes, which may result in involvement beyond skeletal muscles.

Acknowledgments

This work was supported by a grant for Nervous and Mental Disorders from the Ministry of Health, Labour, and Welfare of Japan (15B-4 and 18A-5 to Y.G.); a Grant-in-Aid for Young Scientists (B) from the Ministry of Education, Culture, Sports, Science and Technology (17790738 to M.M.); and a grant from the Comprehensive Research Project on Health Sciences Focusing on Drug Innovation from the Japan Health Sciences Foundation (KHD2207 to Y.G.).

We thank the following attending physicians (all of whom were based in Japan) for referring their patients to us and responding to our follow-up questionnaires: Dr. H. Sasaki (Department of Pediatrics, Kurashiki Central Hospital, Kurashiki, Okayama), Dr. T. Segawa (Department of Pediatrics, Fuji Central Municipal Hospital, Fuji, Shizuoka), Dr. T. Miyajima (Department of Pediatrics, Tokyo Medical University, Shinjuku-ku, Tokyo), Dr. S. Mizukami (Department of Pediatrics, Hakodate Central Hospital, Hakodate, Hokkaido), Dr. H. Koide (Department of Pediatrics, Saitama Medical School Hospital, Saitama), and Dr. Y. Otsuka (Department of Pediatrics, Juntendo University Hospital, Bunkyo-ku, Tokyo).

Potential Conflict of Interest

Nothing to report.

References

1. Robinson BH. Human cytochrome oxidase deficiency. Pediatr Res 2000;48:581–585.
2. DiMauro S, Lombes A, Nakase H, et al. Cytochrome c oxidase deficiency. Pediatr Res 1990;28:536–541.
3. Nonaka I, Koga Y, Shikura K, et al. Muscle pathology in cytochrome c oxidase deficiency. Acta Neuropathol (Berl) 1988;77:152–160.
4. Shoubridge EA. Cytochrome c oxidase deficiency. Am J Med Genet 2001;106:46–52.
5. Sacconi S, Salviati L, Sue CM, et al. Mutation screening in patients with isolated cytochrome c oxidase deficiency. Pediatr Res 2003; 53:224–230.
6. Böhm M, Pronicka E, Karczmarewicz E, et al. Retrospective, multicentric study of 180 children with cytochrome c oxidase deficiency. Pediatr Res 2006;59:21–26.
7. Valnot I, Osmond S, Gigarel N, et al. Mutations of the SCO1 gene in mitochondrial cytochrome c oxidase (COX) deficiency with neonatal-onset hepatic failure and encephalopathy. Am J Hum Genet 2000;67:1104–1109.
8. Papadopoulou LC, Sue CM, Davidson MM, et al. Fatal infantile cardioencephalomyopathy with COX deficiency and mutations in SCO2, a COX assembly gene. Nat Genet 1999;23:333–337.
9. Valnot I, von Kleist-Retzow JC, Barrientos A, et al. A mutation in the human heme A: farnesyl transferase gene (COX10) causes cytochrome c oxidase deficiency. Hum Mol Genet 2000;9:1245–1249.
10. Antonicka H, Mattman A, Carlson CG, et al. Mutation in COX15 produce a defect in the mitochondrial heme biosynthetic pathway, causing early-onset fatal hypertrophic cardiomyopathy. Am J Hum Genet 2003;72:101–114.
11. Moraes CT, Shanske S, Tritschler H-J, et al. mtDNA depletion with variable tissue expression: a novel genetic abnormality in mitochondrial diseases. Am J Hum Genet 1991;48:492–501.
12. Mazziotta MRM, Ricci E, Bertini E, et al. Fatal infantile liver failure associated with mitochondrial DNA depletion. J Pediatr 1992;121: 896–901.
13. Oldfors A, Sommerland H, Holme E, et al. Cytochrome c oxidase deficiency in infancy. Acta Neuropathol (Berl) 1989;77:267–275.
14. Van Biervliet JP, Bruinvis L, Ketting D, et al. Hereditary mitochondrial myopathy with lactic acidemia, a De Toni-Fanconi-Debré syndrome, and a defective respiratory chain in voluntary striated muscles. Pediatr Res 1977;11:1088–1093.
15. DiMauro S, Nicholson JF, Hays AP, et al. Benign infantile mitochondrial myopathy due to reversible cytochrome c oxidase deficiency. Ann Neurol 1983;14:226–234.
16. Zeviani M, Peterson P, Servidei S, et al. Benign reversible muscle cytochrome c oxidase deficiency: a second case. Neurology 1987; 37:64–67.
17. Servidei S, Bertini E, Vici CD, et al. Benign infantile mitochondrial myopathy due to reversible cytochrome c oxidase deficiency: a third case. Clin Neuropathol 1998;7:209–210.
18. Salo MK, Rapola J, Somer H, et al. Reversible mitochondrial myopathy with cytochrome c oxidase deficiency. Arch Dis Child 1992;67:1033–1035.
19. Suzuki M, Sugie H, Tsurui S, et al. Benign infantile mitochondrial myopathy due to reversible cytochrome c oxidase deficiency: histological and biochemical analysis (in Japanese). No To Hattatsu (Tokyo) 1989;21:543–549.
20. Wada H, Nishio H, Nagaki S, et al. [Benign infantile mitochondrial myopathy caused by reversible cytochrome c oxidase deficiency]. No To Hattatsu (Tokyo) 1996;28:443–447. [Japanese]
21. Horvath R, Kemp JP, Tuppen HAL, et al. Molecular basis of infantile reversible cytocrome c oxidase deficiency myopathy. Brain 2009;132:3165–3174.

22. Muraki K, Nishimura S, Goto Y, et al. The association between haematological manifestation and mtDNA deletions in Pearson syndrome. J Inher Metab Dis 1997;20:697–703.

23. Goto Y, Nishino I, Horai S, Nonaka I. Detection of DNA fragments encompassing the deletion junction of mitochondrial genome. Biochem Biophys Res Commun 1996;222:215–219.

24. Akanuma J, Muraki K, Komaki H, et al. Two pathogenic point mutations exist in the authentic mitochondrial genome, not in the nuclear pseudogene. J Hum Genet 2000;45:337–341.

25. King MP, Attardi G. Human cells lacking mtDNA: repopulation with exogenous mitochondria by complementation. Science 1989; 246:500–503.

26. Yasukawa T, Suzuki T, Suzuki T, et al. Modification defect at anticodon wobble nucleotide of mitochondrial tRNAs Leu (UUR) with pathogenic mutations of mitochondrial myopathy, encephalopathy, lactic acidosis, and stroke-like episodes. J Biol Chem 2000; 275:4251–4257.

27. Varshney U, Lee CP, RajBhandary UL. Direct analysis of aminoacylation levels of tRNAs in vivo. Application to studying recognition of Escherichia coli initiator tRNA mutants by glutaminyl-tRNA synthetase. J Biol Chem 1991;266:24712–24718.

28. Trounce LA, Kim YL, Jun AS, Wallace DC. Assessment of mitochondrial oxidative phosphorylation in patient muscle biopsies, lymphoblasts, and transmitochondrial cell lines. In: Attardi GM, Chomyn A, eds. Methods in enzymology. Vol. 264. San Diego: Academic Press USA, 1996:484–509.

29. Nijtmans LG, Henderson NS, Holt NS. Blue native electrophoresis to study mitochondrial and other protein complexes. Methods 2002;26:327–340.

30. D'Aurelio M, Gajewski CD, Lenaz G, Manfredi G. Respiratory chain supercomplexes set the threshold for respiration defects in human mtDNA mutant cybrids. Hum Mol Genet 2006;15: 19198–19209.

31. Hasegawa H, Matsuoka T, Goto Y, Nonaka I. Strongly succinate dehydrogenase-reactive blood vessels in muscles from patients with mitochondrial myopathy, encephalopathy, lactic acidosis, and stroke-like episodes. Ann Neurol 1991;29:601–605.

32. Jarusalem F, Angelini C, Engel AG, Groover RV. Mitochondrial lipid glycogen (MLG) disease of muscle. A morphologically regressive congenital myopathy. Arch Neurol 1973;29:162–169.

33. Pallanck L, Pak M, Schulman LH. tRNA discrimination in aminoacylation. In: Söll D, RajBhandary U, eds. tRNA: structure, biosynthesis, and function. Washington, DC: American Society for Microbiology, 1995:371–394.

34. Chomyn A, Enrriquez JA, Micol V, et al. The mitochondrial myopathy, encephalopathy, lactic acidosis, and stroke-like episode syndrome-associated human mitochondrial tRNALeu (UUR) mutation causes aminoacylation deficiency and concomitant reduced association of mRNA with ribosomes. J Biol Chem 2000;275: 19198–19209.

35. Yasukawa T, Hino N, Suzuki T, et al. A pathogenic point mutation reduces stability of mitochondrial mutant tRNAIle. Nucleic Acids Res 2000;28:3779–3784.

36. Tritschler HJ, Bonilla E, Lombes A, et al. Differential diagnosis of fatal and benign cytochrome c oxidase-deficient myopathies of infancy: an immunohistochemical approach. Neurology 1991;41: 300–305.

Supplementary Fig 1

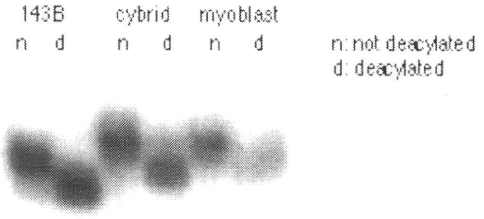

SUPPLEMENTARY INFORMATION

Supplementary Material and Methods

Restriction fragment length polymorphism analysis

To confirm m.14674T>C mutation, the 187-bp PCR fragment with the mismatched and reverse primers was digested by *Bcl I*. If the fragment had m.14674T>C mutation, cleaved fragments of 167 and 20 bps would be obtained. To identify m.14674T>G mutation, we amplified the 541-bp PCR fragment and performed *Nla III* digestion. In the absence of this mutation, cleaved fragments of 408 and 133 bps would be detected; however, if the fragment had m.14674T>G mutation, cleaved fragments of 408 bp would be divided into 242- and 166-bp fragments. Each fragment was detected on a 4% agarose gel and visualized with ethidium bromide under UV light.

Quantification of $tRNA^{Glu}$

Northern blot analysis was performed using total RNA extracted from muscle specimens of patients 2 and 4, from whom a sufficient quantity of RNA was obtained, and from muscle specimens of normal infants (normal controls). Samples of total RNA

were electrophoresed through denaturing 10% polyacrylamide containing 7 M urea. RNA was blotted on a nylon membrane and fixed by UV irradiation. Northern hybridization was then performed using DNA probe specific for mitochondrial tRNA-glutamate ($tRNA^{Glu}$): 5′-ATTCTCGCACGGACTACAACCACGACCAAT-3′ labeled at the 5′ terminus with [γ-^{32}P]ATP (110 TBq/mmol; GE Healthcare Bio-Science, Buckinghamshire, UK). The $tRNA^{Glu}$ amounts were normalized by the amount of mitochondrial tRNA-Leu (UUR) (a probe specific for mitochondrial tRNA-Leu (UUR), 5′-TGTTAAGAAGAGGAATTGAACCTCTGACTG-3′ was used) and nuclear-encoded 5S ribosomal RNA (a probe specific for 5S ribosomal RNA, 5′-GGGTGGTATGGCCGTAGAC-3′ complementary to the 3′ region was used). The DNA probes were labeled at the 5′ terminus with [γ-^{32}P]ATP and T4 polynucleotide kinase (Toyobo, Osaka, Japan). RNAs were quantified by exposing the membrane to an imaging plate on which the radioactivity levels of the bands were measured using a BAS 1000 bioimaging analyzer (Fuji Photo Film, Tokyo, Japan).

Acid polyacrylamide gel electrophoresis analysis

Total RNA samples extracted from cybrids derived from fibroblasts of patient 6

and human osteosarcoma 143B cells (normal control) were prepared under acidic conditions in a cold room and then dissolved in 0.1 M NaOAc (pH 5.0) according to the literature to prevent deacylation [26]. A portion of RNA samples was incubated in a buffer containing 50 mM Tris-HCl (pH 9.5) for complete deacylation of tRNA samples. The same amount of total RNA containing aminoacyl-tRNAs or forcibly deacylated tRNAs in an acid-loading solution were electrophoresed to separate aminoacyl-$tRNA^{Glu}$ and uncharged $tRNA^{Glu}$. RNA was then analyzed by Northern hybridization using the probe specific for mitochondrial $tRNA^{Glu}$:

5′-ATTCTCGCACGGACTACAACCACGACCAAT-3′ labeled at the 5′ terminus with [γ-^{32}P]ATP. The DNA probes were labeled at the 5′ terminus with [γ-^{32}P]ATP and T4 polynucleotide kinase. RNAs were quantified by exposing the membrane to an imaging plate on which the radioactivity levels of the bands were measured using a BAS 1000 bioimaging analyzer.

ELSEVIER

Brain & Development 32 (2010) 171–179

BRAIN & DEVELOPMENT
Official Journal of the Japanese Society of Child Neurology

www.elsevier.com/locate/braindev

Original article

Comprehensive genetic analyses of *PLP1* in patients with Pelizaeus–Merzbacher disease applied by array-CGH and fiber-FISH analyses identified new mutations and variable sizes of duplications

Keiko Shimojima [a], Takehiko Inoue [b], Ai Hoshino [c,d], Satsuki Kakiuchi [e], Yoshiaki Watanabe [f], Masayuki Sasaki [g], Akira Nishimura [g], Akiko Takeshita-Yanagisawa [h], Go Tajima [i], Hiroshi Ozawa [c,j], Masaya Kubota [c,k], Jun Tohyama [l], Masayuki Sasaki [m], Akira Oka [k,n], Kayoko Saito [o], Makiko Osawa [h], Toshiyuki Yamamoto [a,*]

[a] *International Research and Educational Institute for Integrated Medical Sciences (IREIIMS), Tokyo Women's Medical University, 8-1 Kawada-cho, Shinjuku-ward, Tokyo 162-8666, Japan*
[b] *Division of Child Neurology, Institute of Neurological Sciences, Faculty of Medicine, Tottori University, Yonago, Japan*
[c] *Department of Pediatrics, Tokyo Metropolitan Hachioji Children's Hospital, Hachioji, Japan*
[d] *Department of Neuropediatrics, Tokyo Metropolitan Neurological Hospital, Fuchu, Japan*
[e] *Department of Neonatology, Tokyo Metropolitan Bokutoh Hospital, Tokyo, Japan*
[f] *Department of Child Neurology, Okayama University Graduate School of Medicine, Okayama, Japan*
[g] *Department of Pediatrics, Kyoto Prefectural University of Medicine, Kyoto, Japan*
[h] *Department of Pediatrics, Faculty of Medicine, Tokyo Women's medical University, Tokyo, Japan*
[i] *Department of Pediatrics, Hiroshima University Graduate School of Biomedical Sciences, Hiroshima, Japan*
[j] *Shimada Ryoiku Center, Tama, Japan*
[k] *Division of Child Neurology, National Center of Child Health and Development, Tokyo, Japan*
[l] *Epilepsy Center, National Nishi-Niigata Chuo National Hospital, Niigata, Japan*
[m] *Department of Child Neurology, National Center Hospital for Mental, Nervous and Muscular Disorders, National Center of Neurology and Psychiatry, Kodaira, Japan*
[n] *Department of Pediatrics, Faculty of Medicine, The University of Tokyo, Tokyo, Japan*
[o] *Institute of Medical Genetics, Tokyo Women's medical University, Tokyo, Japan*

Received 22 November 2008; received in revised form 2 February 2009; accepted 22 February 2009

Abstract

Pelizaeus–Merzbacher disease (PMD; MIM#312080) is a rare X-linked recessive neurodegenerative disorder. The main cause of PMD is alterations in the proteolipid protein 1 gene (*PLP1*) on chromosome Xq22.2. Duplications and point mutations of *PLP1* have been found in 70% and 10–25% of all patients with PMD, respectively, with a wide clinical spectrum. Since the underlining genomic abnormalities are heterogeneous in patients with PMD, clarification of the genotype-phenotype correlation is the object of this study. Comprehensive genetic analyses using microarray-based comparative genomic hybridization (aCGH) analysis and genomic sequencing were applied to fifteen unrelated male patients with a clinical diagnosis of PMD. Duplicated regions were further analyzed by fiber-fluorescence *in situ* hybridization (FISH) analysis. Four novel and one known nucleotide alterations were identified in five patients. Five microduplications including *PLP1* were identified by aCGH analysis with the sizes ranging from

* Corresponding author. Tel.: +81 3 3353 8111; fax: +81 3 3352 3088
E-mail address: yamamoto@imcir.twmu.ac.jp (T. Yamamoto).

0387-7604/$ - see front matter
doi:10.1016/j.braindev.2009.02.011

374 to 951-kb. The directions of five *PLP1* duplications were further investigated by fiber-FISH analysis, and all showed tandem duplications. The common manifestations of the disease in patients with *PLP1* mutations or duplications in this study were nystagmus in early infancy, dysmyelination revealed by magnetic resonance imaging (MRI), and auditory brain response abnormalities. Although the grades of dysmyelination estimated by MRI findings were well correlated to the clinical phenotypes of the patients, there is no correlation between the size of the duplications and the phenotypic severity.

Keywords: Array-based comparative genomic hybridization (aCGH); Fiber-FISH; Fluorescence *in situ* hybridization (FISH); Pelizaeus–Merzbacher disease (PMD); Proteolipid protein 1 (*PLP1*)

1. Introduction

Pelizaeus–Merzbacher disease (PMD; MIM#312080) is a rare X-linked recessive neurodegenerative disorder characterized by early onset nystagmus and hypotonia later evolving into spastic tetraparesis, dystonia, ataxia, and developmental delay usually beginning in the first year [1–3]. The main cause of PMD is alterations in the proteolipid protein 1 gene (*PLP1*; MIM#300401) on chromosome Xq22.2 [4–6], which encodes 2 proteins, PLP1 and the splicing variant, DM20, both of which are abundantly expressed in oligodendrocytes [3]. PLP1 is thought to play a major role in myelin sheath formation by promoting sheath compaction [7]. Within the heterogeneous group of dysmyelinating disorders, PMD accounts for 6.5% of all cases [8].

It has been proposed that patients with *PLP1*-related inherited dysmyelinating disorders should be clinically divided into 3 subgroups in order of decreasing severity: connatal, classic, and X-linked spastic paraplegia type 2 (SPG2; MIM#312920) [9]. Duplications of *PLP1* can be found in up to 70% of all patients with PMD, indicating that increased *PLP1* dosage is deleterious for normal myelination [10,11]. Point mutations in *PLP1* have been found in 10–25% of PMD cases with the entire clinical spectrum [11], ranging from the most severe connatal form to the least severe SPG2 form, depending on the affected domain of the protein [9]. Although there are characteristic clinical and radiological features of PMD [1,12], molecular and/or cytogenetic analyses are necessary for final diagnosis because *PLP1* is only expressed in the central nervous system and there are no practical biochemical tests available. The first step in genetic testing should be a genomic dosage analysis of *PLP1* because the major genetic aberration is duplication of *PLP1*. For this purpose, various methods have been used, including southern blotting [6], quantitative polymerase chain reaction (PCR) [13], fluorescence *in situ* hybridization (FISH) [14], multiplex ligation-dependent probe amplification (MLPA) [15], and multiplex amplifiable probe hybridization (MAPH) [16]. Recently, microarray-based comparative genome hybridization (aCGH) has emerged as a novel technology that enables detection and determination of the size of the duplicated or deleted genomic intervals [17]. In case of normal dosage of *PLP1*, nucleotide sequences of *PLP1* should be examined [18]. Here, we report our recent studies to develop comprehensive molecular and cytogenetic analyses to diagnose patients with PMD and to understand the pathogenic mechanism of PMD and its correlation between clinical phenotypes.

2. Materials

Fifteen unrelated male patients (age span from 1 year to 20 years old) with congenital dysmyelination were referred to us for genetic diagnosis based on the clinical diagnosis as PMD. Clinical information and radiographic findings by magnetic resonance imaging (MRI) for the patients were obtained from attending doctors. Based on the approval by the ethics committee at the institution, informed consents were obtained from patient's families, and peripheral blood samples were obtained from all patients. Lymphoblast cell lines were established from lymphocytes extracted from peripheral blood samples by immortalization with Epstein-Barr virus. Three of the fifteen patients (P1, P3, P4) had been diagnosed as having *PLP1* duplications by previously performed comparative PCR amplification method (data not shown).

Genomic DNAs of the patients were extracted from peripheral blood samples using the QIAquick DNA Extraction Kit (QIAGEN, Hamburg, Germany). Metaphase or prometaphase chromosomes were prepared from phytohemagglutinin-stimulated peripheral blood lymphocytes or lymphocyte cell lines according to standard techniques.

One extra cell line (S1) that showed duplication of Xp22.31 including steryl-sulfatase precursor gene (*STS*) as determined by aCGH, was derived from a non-PMD mentally retarded patient and used for fiber-FISH analysis as a positive control of *STS* duplication.

Population-based control DNA samples were obtained from 100 healthy Japanese volunteers.

3. Methods

3.1. aCGH analysis

aCGH analysis, using the Human Genome CGH Microarray 105A chip (Agilent Technologies, Santa

Clara, CA), was performed according to the manufacturer's instructions [19]. The data was extracted with Feature Extraction version 9 (Agilent Technologies) and visualized by CGH Analytics version 3.5 (Agilent Technologies). Statistically significant aberrations were determined using the ADM-II algorithm in CGH Analytics version 3.5 (Agilent Technologies).

3.2. Fiber-FISH analysis

Phytohemagglutinin-stimulated lymphocytes or lymphoblasts were harvested using a routine procedure that generates metaphase chromosomes and interphase nuclei. The fiber-FISH slides were prepared as follows: approximately 20 μl of cell suspensions containing metaphase and prometaphase chromosomes were pipetted onto a slide that was then dipped into a 10% sodium dodecyl sulfate (SDS) solution and removed slowly. Bacterial artificial chromosome (BAC) clones were selected from an in-silico library (UCSC Human genome browser, March 2006); RP4-540A13 and RP5-1055C14 mapped to the region surrounding *PLP1*, CTD-2171N231 and RP11-98J1 mapped to the *STS* region of Xp22.31. DNAs from the BAC clones were extracted using GenePrepStar PI-80X (Kurabo, Osaka, Japan), and labeled with digoxigenin-11-dUTP or biotin-16-dUTP (Roche Applied Science, Mannheim, Germany) by nick translation and denatured at 70 °C for 5 min. After hardening process with incubation at 65 °C for 150 min, the chromosome slides were denatured in 70% formamide/2× standard saline citrate (SSC) at 70 °C for 2 min, and then dehydrated at −20 °C in ethanol. The probe-hybridization mixture was applied on the chromosome slides and incubated at 37 °C for more than 16 h. The slides were then washed in 50% formamide/2× SSC at 37 °C for 12 min, 2× SSC at room temperature for 10 min, 1× SSC for 10 min, and 4× SSC for 10 min. And finally, the slides were incubated with 1% bovine serum albumin (BSA), 4× SSC, Fluorescein anti-biotin (Vector, Burlingame, CA, USA) and Anti-digoxigenin-rhodamine, Fab fragments (Roche) at 37 °C for 1 h. Slides were washed 3 times: in 4× SSC for 5 min, in 0.05% Triton-X-100/4× SSC for 5 min with shaking, and finally in 4× SSC for 5 min. The slides were then mounted in antifade solution containing 4′,6-diamino-2-phenylindole (DAPI) stain. Photomicroscopy was performed using a LICA CTR6000 microscope containing a quad filter set with single band excitation filters (Leica Microsystems, Tokyo, Japan).

3.3. PLP1 mutation analysis

The sequence of the patients' 7 coding exons of *PLP1* was determined using the neighboring intronic primers reported by Hobson et al. [20] and a BigDye Terminator Cycle Sequencing kit according to the manufacturer's protocol (Applied Biosystems, Foster City, CA). One hundred control samples were genotyped to verify that the *PLP1* mutation identified in the PMD patients was not found in the general population.

4. Results and discussion

4.1. Genetic diagnosis of PMD

Three distinct genetic mechanisms responsible for PMD have been reported: (1) Loss of PLP1 function caused by null mutations or deletions; (2) gain of toxic function (the PLP1 mutant protein accumulates in the endoplasmic reticulum, triggering increased oligodendrocyte cell death by apoptosis resulting in dysmyelination); (3) overexpression of PLP1 due to genomic duplication [3,7]. As mentioned in Section 2, three (P1, P3, and P4) of the 15 patients had been diagnosed as having *PLP1* duplications by previously performed comparative PCR amplification method, which were re-confirmed by aCGH and fiber-FISH in this study. Subsequently, two (P2 and P5) of the remaining twelve subjects were newly diagnosed as having *PLP1* duplications by aCGH. For the remaining ten patients without genomic duplications, we analyzed the genomic sequence of *PLP1* and identified three missense mutations, one splicing mutation, and one 3-bp deletion (Table 1). Thus, we were unable to determine genetic causes for the phenotype in the remaining five patients, and there is no patient who showed deletion of *PLP1*.

4.2. Detection of genomic duplications of PLP1 by aCGH

aCGH is a revolutionary platform that has been recently adopted in the clinical laboratory. The primary advantage of aCGH is that the array is capable of simultaneously detecting DNA copy changes at multiple loci over the whole genome [21].

In the present study, aCGH analysis identified gains of genomic copy numbers including *PLP1* in five subjects (P1, P2, P3, P4, P5), and the sizes of the chromosomal duplications were 374, 461, 676, 858, and 951-kb, respectively (Table 1 and Fig. 1a). The 461-kb duplication identified in P2 was not detected using standard FISH analysis at another medical facility previously, indicating the advantages of aCGH testing for PMD. There was no genomic copy number aberration in the remaining ten subjects (data not shown). A genomic copy number gain was identified on Xp22.31 with the size of 1.5-Mb in the sample from S1 (Fig. 1b).

4.3. Fiber-FISH analysis

aCGH holds the promise of being the initial diagnostic tool in the identification of visible and submicroscopic

Table 1
Clinical characteristics of the patients with PLP1 duplications or mutations.

	P1	P2	P3	P4	P5	P6	P7	P8	P9	P10
Clinical subtype	Connatal	Classic	Connatal	Connatal	Connatal	Connatal	Connatal	Connatal	Connatal	Connatal
Age at examination	1 year	14 years	20 years	4 months	2 years	2 years	1 year	1 year	4 months	1 year 5 months
Disease onset	1 month	1 day	NA	1 day	1 month	2 months	1 day	1 week	1 month	1 month
Symptoms at onset	Nystagmus	Nystagmus	NA	Nystagmus	Nystagmus Hypotonia	Nystagmus	Asphyxia	Abnormal ABR	Microcephaly*	Nystagmus
Severity score	0	2	0	0	0	0	0	0	0	0
Family history	+	None	NA	None	None	None	None	None	None	None
Age at death				4 years						
Psychomotor development										
Head control	None	7 months	None	None	None	None	None	None	None	None
Sitting	None	4 years	None	None	None	None	None	None	None	None
Walking	None	4 years	None	None	None	None	None	None	None	None
Last evaluation	14 years	14 years	33 years	4 years	2 years	2 years	1 year	4 years	5 months	1 year 5 months
Neurological signs										
Nystagmus	+	+	None	+	+	+	+	+	+	+
Muscular hypotonia	+	None	+	+	+	+ (upper limbs)	+	+	+	+
Pyramidal signs	None	+	+		+	+ (lower limbs)	None	None	None	
Ataxia		+								
Tremor	+									
Seizures				+				+	+	Sensori-neural
deafness										
Other symptoms		Dysarthria		Choreoathetosis			Strider		Microcephaly	
Disease course		Deterioration; now only sitting								
ABR findings	Only I–III waves	Only I–III waves	NA	Only I wave	Only I wave	Only I wave	Only I–III waves	Only I wave	Only I wave	Only I–II waves
MRI findings	Delayed myelination	Incomplete myelination	NA	Hypomyelination	Hypomyelination	Delayed myelination	Delayed myelination	Delayed myelination	Delayed myelination	Hypomyelination
Genotype	Duplication	Duplication	Duplication	Duplication	Duplication	Missense mutation	Missense mutation	Missense mutation	Splicing mutation	Nucleotide deletion
	374-kb	461-kb	676-kb	858-kb	951-kb	exon 2c.149A> G(p.Tyr50Cys)	exon 3c.247G> A(p.Gly83Arg)	exon 3c.254TA> Cp.Leu85Pro	intron 3IVS3-1G>C (splicing error)	exon 3c.238_240delTTC (p.Phe80del)

*, His microcephaly is −3.2SD; NA, not available; MRI, magnetic resonance imaging; ABR, auditory brain response.

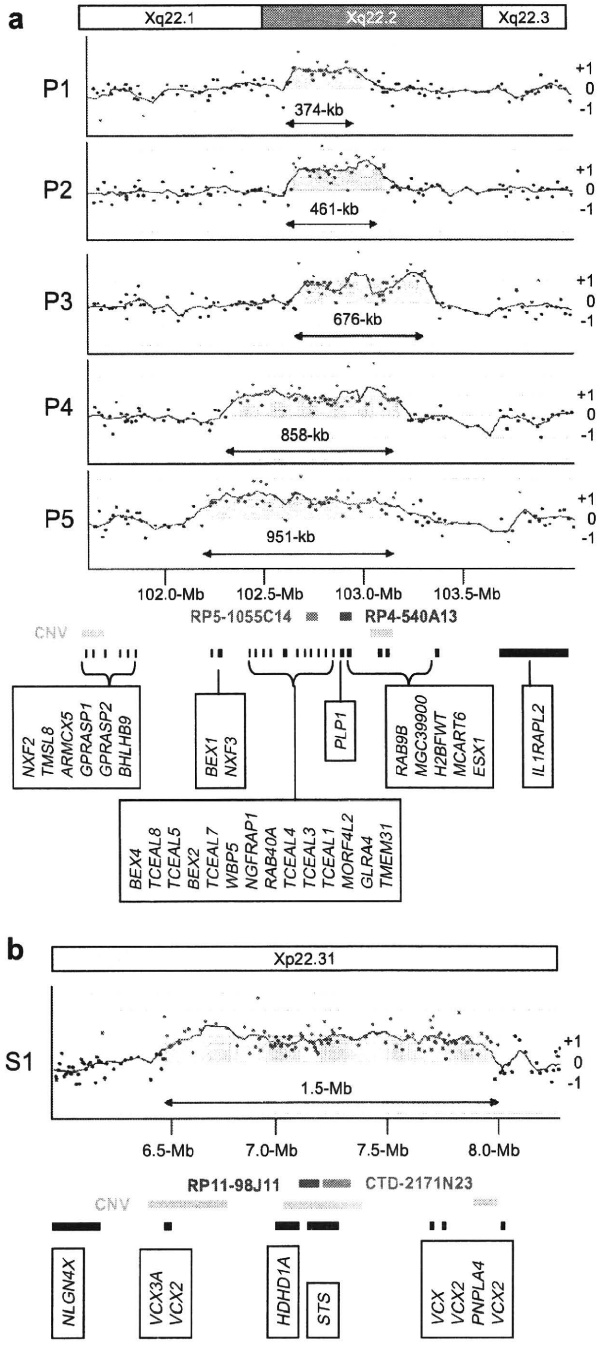

Fig. 1. Results of aCGH. CGH Analytics ver 3.5 (Agilent technologies) visualized genomic copy number aberration on Xq22.2 including *PLP1* (P1, P2, P3, P4, P5) (a) and on Xp22.31 including *STS* (S1) (b). The *X*-axis indicates physical position of chromosome X, and the scales of chromosome bands and physical position were depicted top and bottom, respectively. The *Y*-axis indicates the signal $\log_2$ ratio; positive and negative numbers indicate gain and loss of genomic copy numbers, respectively. The locations of the indicated genes (black rectangles), known copy number variations (CNVs) (orange rectangles), and the two BAC probes used in fiber-FISH analyses with green and red rectangles are shown under the figure depicted on the map according to the scale.

chromosome abnormalities [22], but it does not provide genome position or orientation information. Several cases have been reported in which the duplication is non-contiguous and the additional copy is found in a cytogenetically distinguishable band on the X chromosome (Xq22 and Xq26.3) [23]. Therefore, we should reconfirm the results of aCGH by another method including FISH analysis, especially in case of genetic counseling [23].

We checked the signals by conventional FISH analysis using metaphase, and translocations were denied in all samples (data not shown). Subsequently, two-color fiber-FISH analyses were performed to confirm the directions of the genomic duplications of *PLP1* in the five subjects, and the all duplicated segments were inserted in tandem (Fig. 2). The subjects with the longer duplicated regions (P4 and P5) showed longer intervals between the 2 sets of probe signals, which are consistent with the results of the aCGH analysis (Fig. 1a). The gain of genomic copy number on Xp22.31 in S1 was also analyzed by fiber-FISH, which showed inverted segments (Fig. 2).

Detection and visualization of *PLP1* duplications require specific molecular and cytogenetic technologies. Duplication of chromosomal regions can be determined by FISH analysis as a doublet signal in interphase chromosomes derived from immortalized lymphocyte cell lines [14,24]. However, when the duplicated region is very small and the locations of the duplicated segments are too close to each other, it is difficult to identify signals independently even if we use interphase chromosomes. In such cases, stretched chromatins rather than

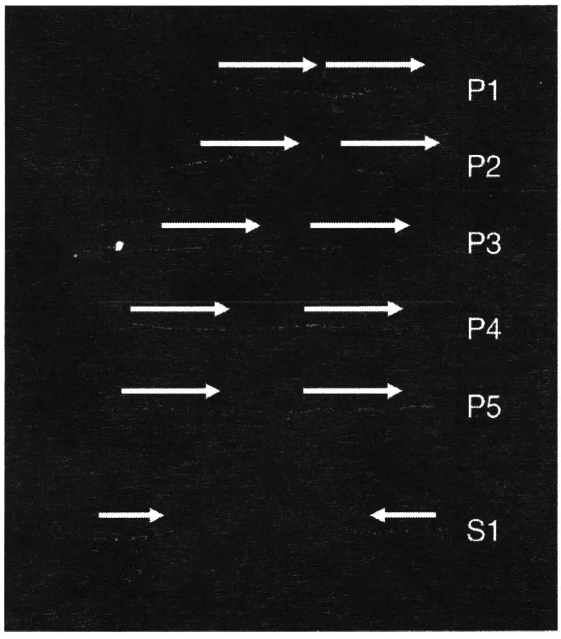

Fig. 2. The results of two-color fiber-FISH analyses. White arrows indicate the direction of duplicated segments.

the conventional interphase or metaphase chromosomes can be used for fiber-FISH analysis [25]. In this technique, two copies of the gene can be visualized as a doublet signal [14].

Interestingly, in PMD patients with *PLP1* duplications, the rearrangement breakpoints for each patient are different, yielding duplicated genomic segments of varying lengths [25–28]. Based on the genomic region around *PLP1*, Woodward et al. suggest that duplicated segments or low copy repeats (LCRs) may promote instability [26]. In this study, the distal ends of the duplicated segments were located in a copy number variation (CNV) region (cnp1417: 102,969,058–103,341,717) [29] in all five subjects, and the proximal ends were differently expanded (Fig. 1a). These findings were similar to the majority of the 11 duplications found by Woodward et al. [26]. Additional studies have shown that *PLP1* duplication events may be stimulated by LCRs or by nonhomologous pairs at both the proximal and distal breakpoints [21]. Despite the variation in size, the duplications encompassing *PLP1* are usually found in tandem [26,30]. All of our subjects with *PLP1* duplications had tandem duplications, as revealed by fiber-FISH analysis (Fig. 2). We also analyzed the region of microduplications of *STS* on Xp22.31, known as the CNV region, by fiver-FISH, which demonstrated that the duplicated segment was inserted in inverted direction (Fig. 2). This indicates that the chromosomal duplication mechanism varies depending on the location.

4.4. *PLP1* mutations

To attempt to identify the genomic anomalies responsible for PMD in the remaining ten patients without *PLP1* duplications, we sequenced all the seven exons of *PLP1* and identified nucleotide alterations in five patients (Table 1, Fig. 3). Three of them were missense mutations, i.e. c.149A>G (p.Tyr50Cys) in exon 2, c.247G>A (p.Gly83Arg) in exon 3, and c.254T>C (p.Leu85Pro) in exon 3, in P6, P7, and P8, respectively. One was a splicing mutation, IVS3-1G>C in intron 3, in P9. Another was 3-bp deletion, c.238_240delCTT (p.Phe80del) in exon 3, in P10. Although c.149A>G was previously reported by Hübner et al. [18], the others were novel.

The two missense substitutions, c.247G>A and c.254T>C, are located within the second hydrophobic transmembrane domain. The nucleotide alteration, IVS3-1G>C, is located within the consensus splicing acceptor site. There is a similar known splicing mutation at the same splicing acceptor site, but it was IVS3-1G>T [31]. As PLP1 is expressed only in the central nervous system, we cannot confirm splicing alterations by RT-PCR. However, the mutations in the consensus splicing sites are believed to cause splicing abnormalities. The other novel 3-bp deletion, c.238_240delTTC, in exon 3 will cause in-frame amino acid deletion. All four novel

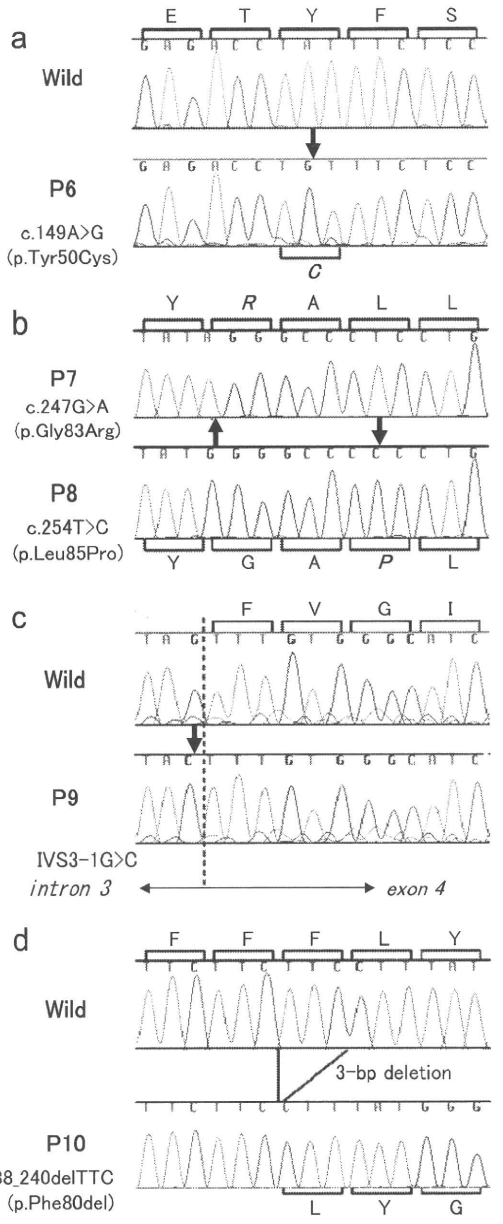

Fig. 3. Partial sequence electrophoregrams of *PLP1* mutations identified in this study. Thick arrows and italic amino acid symbols indicate the positions of mutations and altered amino acids, respectively. The broken line indicates exon–intron boundary (C). wild; sequence of wild type.

mutations were not detected in the 100 control samples, leading us to conclude that these should not be polymorphisms. Because it is well known that the genomic sequence of *PLP1* is highly conserved between species [32], these novel mutations should be pathogenic for patients with PMD. Previously, we reported two pathogenic *PLP1* mutations identified on the patients with the connatal form of PMD, and one of which, jimpy^{msd} mutation, was identical with the mice model [33,34]. Including them, more than 100 *PLP1* mutations have been reported to date (see the GeneTests Web site: http://www.genetests.org). Mutations

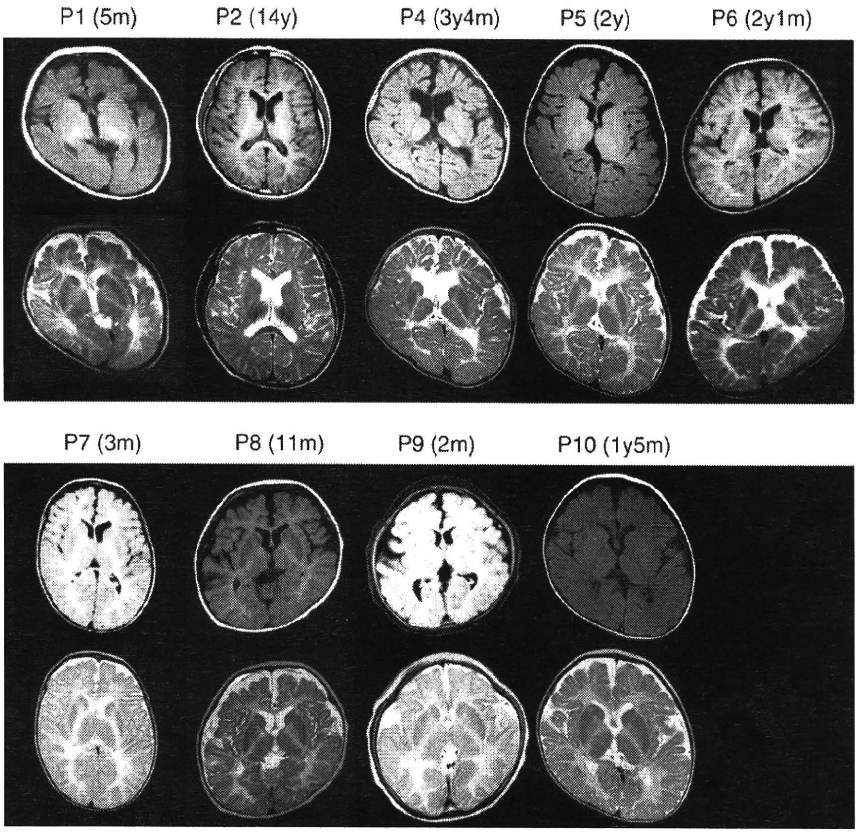

Fig. 4. Brain MRIs of nine patients analyzed in this study. Axial T1- and T2-weighted images are in the top and bottom rows, respectively. Ages at the time of examination are shown in brackets. y; years, m; months.

are distributed throughout all of the *PLP1* coding exons, and each mutation is usually unique to a family [7]. The fact that the majority of *PLP1* missense mutations cause more severe phenotypes than null mutations suggests that the profound dysmyelination resulting from *PLP1* point mutations probably arises not from the absence of functional protein, but rather from a cytotoxic effect of the mutant protein [3].

4.5. Correlation of PLP1 genotypes with PMD phenotypes

The clinical phenotypes of ten subjects who were diagnosed as having *PLP1* duplications (five) or *PLP1* nucleotide alterations (five) are summarized in Table 1. P2 is the only patient with the milder classic form of PMD, and demonstrated the greatest walking ability of all cases in this study. The other subjects were diagnosed with the connatal form of PMD with severe developmental delay. P4 died at age 4, although no details were provided.

Brain MRIs were obtained from nine patients and shown in Fig. 4. All of them showed abnormal intensity in the white matter. Although P2 showed normal high intensity in T1-weighted image (T1), that of the frontal lobe in T2-weighted image (T2) is higher than that of the occipital. This indicated incomplete myelination. P6, P7, P8, and P9 showed high intensity in both T1 and T2, indicating delayed myelination. P1 showed low intensity in T1, and high intensity in T2. As these MRIs were obtained when he was 5 months old, this indicated delayed myelination. P4, P5, and P10 showed low intensity in T1, and high intensity in T2, indicating very severe hypomyelination.

All ten patients having a *PLP1* mutation or duplication showed nystagmus in early infancy, dysmyelination revealed by MRI, and auditory brain response (ABR) abnormalities (Table 1). This triad of presenting symptoms should be the clue to get a clinical diagnosis of PMD. Regarding the radiological findings of the patients, all the provided MRI findings showed dysmyelination with varying degrees (Fig. 4). P4 with the most severe phenotype of PMD showed very low intensity white matter in the T1-weighted imaging, whereas P2 with the mildest form of PMD showed only mildly affected incomplete myelination in T2-weighted imaging. These MRI findings are well-correlated with the clinical severity.

All five patients with nucleotide alterations in *PLP1* displayed the very severe connatal type PMD, whereas P2 whose genome contained a small duplication including *PLP1* showed the milder classical type PMD. These results agree with previous reports showing that the phe-

notypes of patients with genomic duplications are generally milder than those with nucleotide mutations [3]. However, the other four patients with *PLP1* duplications, P1, P3, P4, and P5, displayed the severe connatal form of PMD.

P4 showed a large duplicated region and died when he was 4 years old. On the other hand, P1 contained a very small duplicated segment, similar to P2 in the length, but displayed a very severe phenotype. Thus, it appears that, as suggested by Regis et al., the extent of the duplicated genomic segments does not correlate with clinical severity [35].

According to Lee et al., 65% of patients with *PLP1* duplications have complex rearrangements in nucleotide sequence levels [28]. In this study, we detected *PLP1* duplications by aCGH, and the directions of those duplicated regions were determined by fiber-FISH. However, there is still the possibility that more complicated small rearrangements exist in the duplicated region, particularly in P1. The existence of more complicated rearrangements may explain the reason why there is no correlation between the size of the duplication and the phenotypic severity.

4.6. Differential diagnosis

After genetic evaluation of *PLP1*, the five patients, who did not show any mutations in *PLP1*, were re-evaluated, and one of them was diagnosed as having metachromatic leukodystrophy in the other institution. Another patient showed congenital leukodystrophy with migrating partial seizures in infancy, but no nystagmus and no ABR abnormality, indicating that PMD would be misdiagnosis. Since the other three patients fulfilled the triad described above, the disease-causing mutations might be on the non-coding upstream region of PLP1, or on the other candidate genes for congenital leukodystrophy, including the gap junction protein α12 (GJA12) and others [36,37].

Acknowledgements

This work was supported by the International Research and Educational Institute for Integrated Medical Sciences, Tokyo Women's Medical University, which is supported by the Program for Promoting the Establishment of Strategic Research Centers, Special Coordination Funds for Promoting Science and Technology, Ministry of Education, Culture, Sports, Science and Technology (Japan).

References

[1] Boulloche J, Aicardi J. Pelizaeus–Merzbacher disease: clinical and nosological study. J Child Neurol 1986;1:233–9.
[2] Koeppen AH, Robitaille Y. Pelizaeus–Merzbacher disease. J Neuropathol Exp Neurol 2002;61:747–59.
[3] Inoue K. PLP1-related inherited dysmyelinating disorders: Pelizaeus–Merzbacher disease and spastic paraplegia type 2. Neurogenetics 2005;6:1–16.
[4] Hudson LD, Puckett C, Berndt J, Chan J, Gencic S. Mutation of the proteolipid protein gene PLP in a human X chromosome-linked myelin disorder. Proc Natl Acad Sci USA 1989;86:8128–31.
[5] Gencic S, Abuelo D, Ambler M, Hudson LD. Pelizaeus–Merzbacher disease: an X-linked neurologic disorder of myelin metabolism with a novel mutation in the gene encoding proteolipid protein. Am J Hum Genet 1989;45:435–42.
[6] Ellis D, Malcolm S. Proteolipid protein gene dosage effect in Pelizaeus–Merzbacher disease. Nat Genet 1994;6:333–4.
[7] Garbern JY. Pelizaeus–Merzbacher disease: genetic and cellular pathogenesis. Cell Mol Life Sci 2007;64:50–65.
[8] Heim P, Claussen M, Hoffmann B, Conzelmann E, Gartner J, Harzer K, et al. Leukodystrophy incidence in Germany. Am J Med Genet 1997;71:475–8.
[9] Cailloux F, Gauthier-Barichard F, Mimault C, Isabelle V, Courtois V, Giraud G, et al. Genotype-phenotype correlation in inherited brain myelination defects due to proteolipid protein gene mutations. Clinical European network on brain dysmyelinating disease. Eur J Hum Genet 2000;8:837–45.
[10] Sistermans EA, de Coo RF, De Wijs IJ, Van Oost BA. Duplication of the proteolipid protein gene is the major cause of Pelizaeus–Merzbacher disease. Neurology 1998;50:1749–54.
[11] Mimault C, Giraud G, Courtois V, Cailloux F, Boire JY, Dastugue B, et al. Proteolipoprotein gene analysis in 82 patients with sporadic Pelizaeus–Merzbacher disease: duplications, the major cause of the disease, originate more frequently in male germ cells, but point mutations do not. The clinical European network on brain dysmyelinating disease. Am J Hum Genet 1999;65:360–9.
[12] Caro PA, Marks HG. Magnetic resonance imaging and computed tomography in Pelizaeus–Merzbacher disease. Magn Reson Imaging 1990;8:791–6.
[13] Inoue K, Osaka H, Sugiyama N, Kawanishi C, Onishi H, Nezu A, et al. A duplicated PLP gene causing Pelizaeus–Merzbacher disease detected by comparative multiplex PCR. Am J Hum Genet 1996;59:32–9.
[14] Woodward K, Kendall E, Vetrie D, Malcolm S. Pelizaeus–Merzbacher disease: identification of Xq22 proteolipid-protein duplications and characterization of breakpoints by interphase FISH. Am J Hum Genet 1998;63:207–17.
[15] Wolf NI, Sistermans EA, Cundall M, Hobson GM, Davis-Williams AP, Palmer R, et al. Three or more copies of the proteolipid protein gene PLP1 cause severe Pelizaeus–Merzbacher disease. Brain 2005;128:743–51.
[16] Combes P, Bonnet-Dupeyron MN, Gauthier-Barichard F, Schiffmann R, Bertini E, Rodriguez D, et al. PLP1 and GPM6B intragenic copy number analysis by MAPH in 262 patients with hypomyelinating leukodystrophies: identification of one partial triplication and two partial deletions of PLP1. Neurogenetics 2006;7:31–7.
[17] Lee JA, Cheung SW, Ward PA, Inoue K, Lupski JR. Prenatal diagnosis of PLP1 copy number by array comparative genomic hybridization. Prenat Diagn 2005;25:1188–91.
[18] Hubner CA, Orth U, Senning A, Steglich C, Kohlschutter A, Korinthenberg R, et al. Seventeen novel PLP1 mutations in patients with Pelizaeus–Merzbacher disease. Hum Mutat 2005;25:321–2.
[19] Bartocci A, Striano P, Mancardi MM, Fichera M, Castiglia L, Galesi O, et al. Partial monosomy Xq(Xq23 –> qter) and trisomy 4p(4p15.33 –> pter) in a woman with intractable focal epilepsy, borderline intellectual functioning, and dysmorphic features. Brain Dev 2008;30:425–9.
[20] Hobson GM, Davis AP, Stowell NC, Kolodny EH, Sistermans EA, de Coo IF, et al. Mutations in noncoding regions of the proteolipid protein gene in Pelizaeus–Merzbacher disease. Neurology 2000;55:1089–96.

[21] Bejjani BA, Shaffer LG. Application of array-based comparative genomic hybridization to clinical diagnostics. J Mol Diagn 2006;8:528–33.
[22] Shaffer LG, Bejjani BA. Medical applications of array CGH and the transformation of clinical cytogenetics. Cytogenet Genome Res 2006;115:303–9.
[23] Woodward K, Cundall M, Palmer R, Surtees R, Winter RM, Malcolm S. Complex chromosomal rearrangement and associated counseling issues in a family with Pelizaeus–Merzbacher disease. Am J Med Genet A 2003;118A:15–24.
[24] Inoue K, Kanai M, Tanabe Y, Kubota T, Kashork CD, Wakui K, et al. Prenatal interphase FISH diagnosis of PLP1 duplication associated with Pelizaeus–Merzbacher disease. Prenat Diagn 2001;21:1133–6.
[25] Inoue K, Osaka H, Imaizumi K, Nezu A, Takanashi J, Arii J, et al. Proteolipid protein gene duplications causing Pelizaeus–Merzbacher disease: molecular mechanism and phenotypic manifestations. Ann Neurol 1999;45:624–32.
[26] Woodward KJ, Cundall M, Sperle K, Sistermans EA, Ross M, Howell G, et al. Heterogeneous duplications in patients with Pelizaeus–Merzbacher disease suggest a mechanism of coupled homologous and nonhomologous recombination. Am J Hum Genet 2005;77:966–87.
[27] Lee JA, Inoue K, Cheung SW, Shaw CA, Stankiewicz P, Lupski JR. Role of genomic architecture in PLP1 duplication causing Pelizaeus–Merzbacher disease. Hum Mol Genet 2006;15:2250–65.
[28] Lee JA, Carvalho CM, Lupski JR. A DNA replication mechanism for generating nonrecurrent rearrangements associated with genomic disorders. Cell 2007;131:1235–47.
[29] Redon R, Ishikawa S, Fitch KR, Feuk L, Perry GH, Andrews TD, et al. Global variation in copy number in the human genome. Nature 2006;444:444–54.
[30] Inoue K. Pelizaeus–Merzbacher disease and spastic paraplegia type 2. In: Lupski JR, Stankiewicz P, editors. Genomic disorders. Totowa, NJ: Humana press; 2006. p. 263–9.
[31] Strautnieks S, Malcolm S. A G to T mutation at a splice site in a case of Pelizaeus–Merzbacher disease. Hum Mol Genet 1993;2:2191–2.
[32] Diehl HJ, Schaich M, Budzinski RM, Stoffel W. Individual exons encode the integral membrane domains of human myelin proteolipid protein. Proc Natl Acad Sci USA 1986;83:9807–11.
[33] Yamamoto T, Nanba E, Zhang H, Sasaki M, Komaki H, Takeshita K. Jimpy(msd) mouse mutation and connatal Pelizaeus–Merzbacher disease. Am J Med Genet 1998;75:439–40.
[34] Yamamoto T, Nanba E. A novel mutation (A246T) in exon 6 of the proteolipid protein gene associated with connatal Pelizaeus–Merzbacher disease. Hum Mutat 1999;14:182.
[35] Regis S, Biancheri R, Bertini E, Burlina A, Lualdi S, Bianco MG, et al. Genotype-phenotype correlation in five Pelizaeus–Merzbacher disease patients with PLP1 gene duplications. Clin Genet 2008;73:279–87.
[36] Uhlenberg B, Schuelke M, Ruschendorf F, Ruf N, Kaindl AM, Henneke M, et al. Mutations in the gene encoding gap junction protein alpha 12 (connexin 46.6) cause Pelizaeus–Merzbacher-like disease. Am J Hum Genet 2004;75:251–60.
[37] Henneke M, Combes P, Diekmann S, Bertini E, Brockmann K, Burlina AP, et al. GJA12 mutations are a rare cause of Pelizaeus–Merzbacher-like disease. Neurology 2008;70:748–54.